Available online at www.sciencedirect.com
SCIENCE DIRECT
Bioorganic & Medicinal Chemistry Letters
ELSEVIER
Bioorganic & Medicinal Chemistry Letters 14 (2004) 1629–1632

Femtosecond time-resolved guanine oxidation in acridine modified alanyl peptide nucleic acids

D. Weicherding,[a] W. B. Davis,[b,†] S. Hess,[b,‡] T. von Feilitzsch,[b] M. E. Michel-Beyerle[b,*] and U. Diederichsen[a,*]

[a]*Institut für Organische und Biomolekulare Chemie, Universität Göttingen, Tammannstr. 2, D-37077 Göttingen, Germany*
[b]*Institut für Physikalische und Theoretische Chemie, TU-München, Lichtenbergstr. 4, D-85748 Garching, Germany*

Received 27 October 2003; revised 22 January 2004; accepted 23 January 2004

Abstract—Alanyl peptide nucleic acids have been designed to generate linear and rigid pairing complexes. Femtosecond time resolved electron transfer dynamics studies of alanyl–PNA double strands where both strands contain an intercalated 9-amino-6-chloro-2-methoxy-acridine in its protonated state reveal a strong similarity to nearest neighbor interstrand/intrastrand guanine oxidation in the corresponding B-DNA fragment. This observation implies that the combined influence of electronic couplings and energetic parameters, driving force and reorganization energy, on electron transfer dynamics is similar in both structures. With respect to the alanyl–PNA structure, this result is consistent with the notion of stacking distances in the nucleobase staple similar to the one in B-DNA and thus provides additional structural evidence for nucleobase stacking in alanyl–PNA double strands.

1. Introduction

Charge transfer and transport in DNA is still a lively research area,[1–4] even though there was significant progress towards understanding of mechanisms within past years. The observation of long range (~200 Å) hole transport in duplex DNA[5] led to descriptions within models resting on incoherent, thermally activated hopping steps. With a few exceptions,[6] so far direct dynamic information has been accessible only for unistep, short range (<12 Å) hole injection. These experiments are based on modified helical DNA double strands, where excited chromophores, intercalated or capped, are used to oxidize guanine or its analogues separated from the injector by one or more A–T base pairs which serve as superexchange mediators. Depending on the nature and binding conditions of the chromophore, attenuation parameters for the unistep oxidation rate of guanine or its analogues vary from 0.6–0.8 $Å^{-1}$ to 1.5 $Å^{-1}$ and values exceeding 2.0 $Å^{-1}$.[1d,3a,e] This large span has been shown to be caused by the increase of activation energy and, in particular, of the reorganization energy with increasing donor/acceptor distance.[3f] These insights into the combined effects of distance dependent electronic couplings and energetic parameters are complemented by the recent discussion of the role of gating these parameters by structural fluctuations.[2c,7] Since fluctuations are expected to depend on the conformational freedom of the duplex, it is one of the goals of this paper to study hole injection into artificial oligonucleotide like double strands which form linear and rigid pairing complexes. Since such systems allow at the same time for a unique variation of structural parameters, their potential qualification for electron transfer studies is of major interest.

In recent years such an artificial system has been introduced with the alanyl peptide nucleic acid (alanyl–PNA) which is structurally based on a regular alanyl peptide backbone with alternating configuration of the amino acids.[8] Nucleobases are covalently linked to the side chains in β-positions (Fig. 1). Consequently, all nucleobases are oriented on one side of the backbone with a distance of about 3.6 Å, which is close to the stacking distance of 3.4 Å in a B-DNA double helix. Due to this geometry alanyl–PNA forms linear and rigid pairing complexes based on electrostatic and π–π interactions

Keywords: Acridine; Guanine oxidation; Electron transfer; Peptide nucleic acid.
* Corresponding authors. Tel.: +49-551-39-3221; fax: +49-551-39-2944 (U.D.); tel.: +49-89-289-13400; fax: +49-89-289-13026 (M.E.M.-B.); e-mail: Michel-Beyerle@ch.tum.de; udieder@gwdg.de
† Present address: School of Molecular Biosciences, Washington State University, Pullman, WA 99164-4660, USA.
‡ Present address: BASF, Ludwigshafen, Germany.

0960-894X/$ - see front matter © 2004 Elsevier Ltd. All rights reserved.
doi:10.1016/j.bmcl.2004.01.068

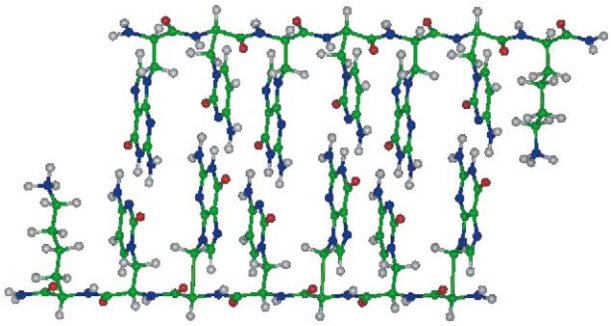

Figure 1. Model of a linear guanine–cytosine pairing alanyl–PNA double strand.

and hydrogen bonding.[9,10] Furthermore, the linear topology allows a variety of pairing modes like Watson–Crick, Hoogsteen and their respective reverse base pairing modes.

In this paper, synthesis and steady state characterization of a variety of self pairing alanyl–PNA oligomers is presented as well as time resolved electron transfer experiments using a widely studied covalently attached acridine derivative as electron acceptor.[3a,d–f]

2. Synthesis and characterization

In order to allow defined stacking of the acridine chromophore within the nucleobase stack, without conformational reorganization of the double strand, 9-amino-6-chloro-2-methoxyacridine (Acr^+) covalently linked to an ornithine side chain was incorporated into alanyl–PNA oligomers instead of one nucleo amino acid.[11] This substitution of nucleobases with Acr^+ leads to further stabilization of the double strands: Double strand formation of self pairing hexamer H-(AlaG-AlaG-AlaC-AlaG-AlaC-AlaC)-Lys-NH_2 (**1**)[12] with a stability of $T_m = 39\,^{\circ}C$ (15% hyperchromicity (H), 6 μM) measured by temperature dependent UV-spectroscopy is based on six G–C base pairs in the reversed Watson–Crick mode (Fig. 2). Substitution of a central guaninyl nucleo amino acid with Acr^+ leads to the selfpairing oligomer H-(AlaG-AlaG-AlaC-Acr-AlaC-AlaC)-Lys-NH_2 (**2**) with an increased stability of $T_m = 52\,^{\circ}C$ (35% H, 6 μM). A comparable stabilization was observed for the A–T pairing oligomers H-(AlaA-AlaA-AlaT-AlaA-AlaT-AlaT)-Lys-NH_2 (**3**, $T_m = 25\,^{\circ}C$, 14% H, 6 μM) and H-(AlaA-AlaA-AlaT-Acr-AlaT-AlaT)-Lys-NH_2 (**4**, $T_m = 37\,^{\circ}C$, 30% H, 6 μM).

Figure 2. G–C and A–T pairing alanyl–PNA double strands with and without 9-amino-6-chloro-2-methoxy-acridine modification (Acr). The letters G, A, C and T symbolize the respective nucleo amino acids.

In order to study distance dependence of guanine oxidation in analogy to previous work on the DNA duplex,[3e,f] other alanyl–PNA oligomers, H-(AlaT-AlaA-AlaT-AlaG-Acr-AlaT)-Lys-NH_2 (**5**) and H-(AlaT-AlaA-AlaG-AlaA-Acr-AlaT)-Lys-NH_2 (**6**), were synthesized. The stabilities of the respected self pairing complexes of oligomers **5** ($T_m = 31\,^{\circ}C$, 20% H, 6 μM) and **6** ($T_m = 30\,^{\circ}C$, 32% H, 6 μM) turned out to be already so high that pairing with complementary strands was prohibited. Even self pairing of oligomers **5** and **6** is strong, the binding conditions are undefined.

Figure 3 shows absorption, fluorescence and fluorescence excitation spectra of Acr^+ in the self-pairing complex **2**. The characteristics are maintained in the complexes **4**, **5** and **6**. The maxima of the absorption at 425 nm and 445 nm are nearly at the same wavelength as reported for analogous DNA duplexes (13 bp and 21 bp).[3d–f] Although the two Acr^+ are adjacent, there is indication of dimer formation.

3. Charge transfer dynamics

Electron transfer from guanine to the singlet excited state of Acr^+ in earlier work has been shown to reduce the fluorescence lifetime.[3a,d–f] Similarly, guanine oxidation is responsible for the fast decay of time resolved fluorescence in strand **2** as compared to strand **4** (Fig. 4). Whereas the fluorescence lifetime (~10 ns) of the A–T oligomer **4** is attributed to the lifetime of the unquenched dye, the decay of the G–C oligomer **2** is much faster (strong component of 290 ps), consistent with electron transfer from guanine to $^1(Acr^+)^*$.

Since these time correlated single photon counting measurements only possess a time resolution of 30 ps and, in addition, cannot follow the population of product states, femtosecond transient absorption experiments have been performed as shown in Figure 5. In these experiments oligomer **2** was excited by a pump pulse at 450 nm with a duration of 150 fs. A second, equally short, laser pulse (probe pulse) with a different,

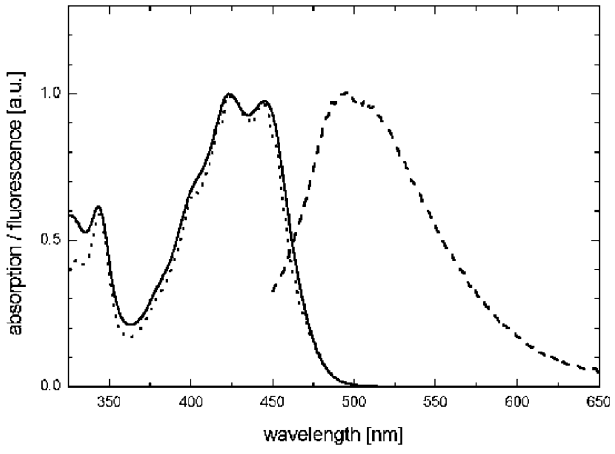

Figure 3. Normalized steady state absorption (solid), fluorescence (dashed), and fluorescence excitation (dotted) spectra of Acr^+ in oligomer **2**.

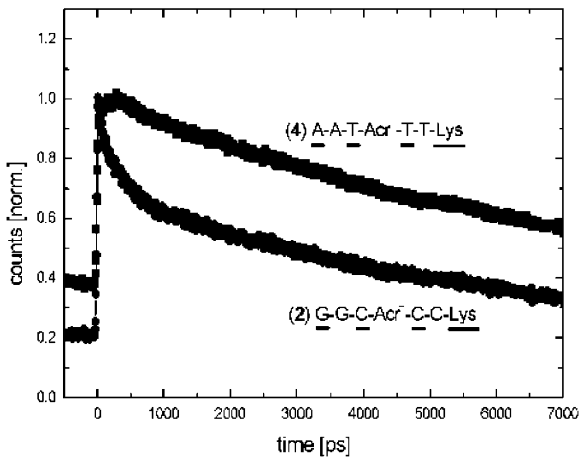

Figure 4. Time resolved fluorescence decay measured by time correlated single photon counting (TCSPC) at 500 nm of Acr^+ containing oligomers **2** and **4** after excitation at 445 nm.

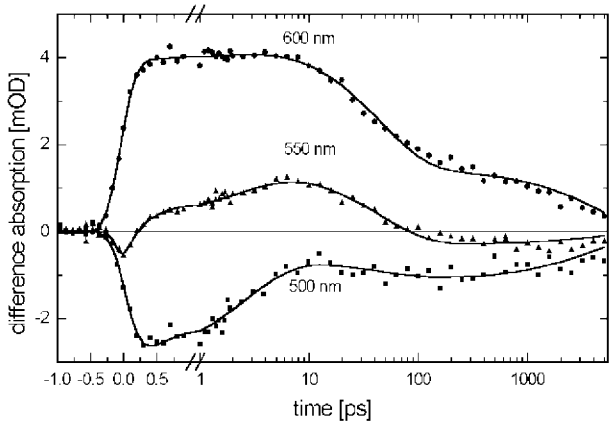

Figure 5. Time resolved absorption traces of oligomer **2** after excitation at 450 nm (logarithmic scale after axis break at 1 ps).

adjustable wavelength and a variable temporal delay was used to follow the absorbance of the sample at well defined time intervals after excitation. Thus, it is possible to follow the decay of the excited state, the formation of transients, and the recovery of the ground state.

Three different processes contribute to the signals shown in Figure 5: (a) Stimulated emission from $^1(Acr^+)^*$ leading to a negative difference absorption signal. (b) Excited state absorption of $^1(Acr^+)^*$ giving rise to a positive signal with the same dynamic features as stimulated emission. (c) Absorption of the neutral radical $Acr^{\cdot}$, also leading to a positive signal. Monitoring at 500 nm, the signal is dominated by stimulated emission as concluded from its negative sign. Although it is superimposed by both $Acr^{\cdot}$ and $^1(Acr^+)^*$ absorption. At 550 nm, the contribution of stimulated emission signal is weak and the signal is dominated by both excited state and radical absorption, whereas at 600 nm, $^1(Acr^+)^*$ and $Acr^{\cdot}$ absorptions occur.

Global fitting of the multiexponential traces presented in Figure 5 revealed three time constants: τ_1 with 3 ps, τ_2 with 46 ps and τ_3 with 4 ns. The amplitudes related to these time constants depend on the wavelength of the probe pulse. Probing at 500 nm yields $A_1 = -2.3$, $A_2 = 0.5$ and $A_3 = -1.1$, probing at 550 nm $A_1 = -1.2$, $A_2 = 1.7$ and $A_3 = -0.3$ as well as additional component at the limit of time resolution which is an experimental artifact, probing at 600 nm $A_1 = -0.5$, $A_2 = 3.0$ and $A_3 = 1.5$. The time constants τ_1 and τ_2 can be assigned to the formation and decay of the radical pair state and are a fingerprint of the forward and back hole transfer rates ($k_1 = (\tau_1)^{-1}$) and ($k_2 = (\tau_2)^{-1}$) as shown in Figure 6. The long component (4 ns, A: 30%) indicates a subpopulation of $^1(Acr^+)^*$ which is due to a defect structure with a hole transfer rate on the order of the lifetime of $^1(Acr^+)^*$ based on the fluorescence decay pattern of oligomer **2** in Figure 4.

In contrast to strands **2** and **4**, time traces of femtosecond difference absorption on oligomers **5** and **6** could not be fit by a multiexponential pattern. This observation supports the notion of undefined self pairing as concluded from the low melting temperatures.

In principle, the predominant ET transfer times of 3 ps and 46 ps in oligomer **2** may reflect forward and back electron transfer between an excited acridine chromophore and either (i) a guanine located on the counterstrand or (ii) a guanine on the same strand with a cytosine as superexchange mediator. We examine both of these possibilities below.

(i) Since these rates resemble the kinetic pattern of guanine oxidation in nearest neighbor Acr^+-G DNA sequences, interstrand nearest neighbor oxidation of guanine seems to also prevail in alanyl–PNA **2**. In fact, depending on the transfer direction (higher rates for transfer in 5′-direction) the nearest neighbor oxidation rates in B DNA range from $(3.8\ ps)^{-1}$ to $(5.9\ ps)^{-1}$ for k_1 and from $(34\ ps)^{-1}$ to $(50\ ps)^{-1}$ for k_2.[3f] In addition, due to the almost symmetrical intercalation of the injector into DNA, the rates for nearest neighbor guanine oxidation are almost invariant for intra- and interstrand processes. The assignment of the kinetic pattern in Figure 6 to interstrand guanine oxidation implies that the combined influence of electronic interactions, driving force and reorganization energy yields identical ET rates in alanyl–PNA and B-DNA.

(ii) With respect to the probability of intrastrand ET in **2** across cytosine, both intra- and interstrand electron transfer from guanine to excited Acr^+ across one A–T base pair (or hypothetically across C which is almost isoenergetic in B-DNA)[13,14] is by three orders of mag-

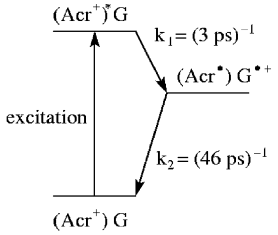

Figure 6. Hole injection and recombination after photoexcitation of Acr^+.

nitude slower than the direct nearest neighbor process.[3e] This drastic distance dependence has been shown to be due to the superposition of two effects, the distance dependent decrease of the superexchange mediated electronic couplings and, far more important in the case of B-DNA, the distance dependent increase of the activation energy caused by an increase of the medium reorganization energy with increasing donor/acceptor separation.[3f] Thus, in case the ET kinetics observed for system **2** would predominantly reflect intrastrand guanine oxidation involving cytosine as superexchange mediator, this interpretation would necessarily imply larger intrastrand electronic couplings and driving force accompanied by smaller reorganization energy as compared to B-DNA. However, even in the limit of the fastest possible electron transfer process (activationless), the measured rate k_1 would be approximately by a factor of 10 too fast as compared with a rate in the hypothetical system Acr^+-C-G in B-DNA. An electronic interaction between Acr^{+*} and guanine in alanyl–PNA which is by at least a factor of 3 larger than in B-DNA appears to be rather improbable as it would need a significantly denser packing of the nucleobase stack as compared to B-DNA.

4. Summary

Oxidation dynamics of guanine in alanyl–PNA structures initiated by intercalated Acr^+ in its excited singlet state is similar to nearest neighbor intra- and interstrand processes in B-DNA. This observation implies that the combined influence of electronic couplings and energetic parameters, driving force and reorganization energy, is similar in both structures modified by intercalated protonated 9-amino-6-chloro-2-methoxy-acridine. With respect to the alanyl–PNA structure this result is consistent with a nucleobase staple of double strands showing similar stacking distances as in B-DNA.

Acknowledgements

Financial support by Volkswagenstiftung is gratefully acknowledged.

References and notes

1. (a) Murphy, C. J.; Arkin, M. R.; Yenkins, Y.; Ghatlia, N. D.; Bossmann, S. H.; Turro, N. J.; Barton, J. K. *Science* **1993**, 1025. (b) Meggers, E.; Michel-Beyerle, M. E.; Giese, B. *J. Am. Chem. Soc.* **1998**, *120*, 12950. (c) Harriman, A. *Angew. Chem., Int. Ed.* **1999**, *38*, 945. (d) Lewis, F. D.; Liu, X.; Liu, J.; Miller, S. E.; Hayes, R. T.; Wasielewski, M. R. *Nature* **2000**, *406*, 51. (e) Shafirovich, V.; Dourandin, A.; Huang, W.; Luneva, N. P.; Geacintov, N. E. *Phys. Chem. Chem. Phys.* **2000**, *2*, 4399. (f) Yoshioka, Y.; Kitagawa, Y.; Takano, Y.; Yamaguchi, K.; Nakamura, T.; Nakatani, K.; Dohno, C.; Saito, I. *J. Am. Chem. Soc.* **2000**, *122*, 5893.
2. (a) Turro, N. J.; Barton, J. K. *J. Biol. Inorg. Chem.* **1998**, *3*, 201. (b) Giese, B. *Acc. Chem. Res.* **2000**, *33*, 631. (c) Schuster, G. B. *Acc. Chem. Res.* **2000**, *33*, 253. (d) Lewis, F. D.; Letsinger, R. L.; Wasielewski, M. R. *Acc. Chem. Res.* **2001**, *34*, 159.
3. (a) Fukui, K.; Tanaka, K. *Angew. Chem.* **1998**, *110*, 167. (b) Fukui, K.; Tanaka, K.; Fujitsuka, M.; Watanabe, A.; Ito, O. *J. Photochem. Photobiol., B* **1999**, *50*, 18. (c) Wan, C.; Fiebig, T.; Schiemann, O.; Barton, J. K.; Zewail, A. H. *Proc. Natl. Acad. Sci. U.S.A.* **2000**, *97*, 14052. (d) Davis, W. B.; Naydenova, I.; Haselsberger, R.; Ogrodnik, A.; Giese, B.; Michel-Beyerle, M. E. *Angew. Chem., Int. Ed.* **2000**, *39*, 2649. (e) Hess, S.; Götz, M.; Davis, W. B.; Michel-Beyerle, M. E. *J. Am. Chem. Soc.* **2001**, *123*, 10046. (f) Davis, W. B.; Hess, S.; Naydenova, I.; Haselsberger, R.; Ogrodnik, A.; Newton, M. D.; Michel-Beyerle, M. E. *J. Am. Chem. Soc.* **2002**, *124*, 2422.
4. (a) Jortner, J.; Bixon, M.; Langenbacher, T.; Michel-Beyerle, M. E. *Proc. Natl. Acad. Sci. U.S.A.* **1998**, *95*, 12759. (b) Berlin, Y. A.; Burin, A. L.; Ratner, M. A. *J. Phys. Chem. A* **2000**, *104*, 443. (c) Bixon, M.; Giese, B.; Wessely, S.; Langenbacher, T.; Michel-Beyerle, M. E.; Jortner, J. *Proc. Natl. Acad. Sci. U.S.A.* **1999**, *96*, 11713. (d) Bixon, M.; Jortner, J. *J. Phys. Chem. B* **2000**, *104*, 3906. (e) Voityuk, A. A.; Jortner, J.; Bixon, M.; Rösch, N. *Chem. Phys. Lett.* **2000**, *324*, 430. (f) Voityuk, A. A.; Rösch, N.; Bixon, M.; Jortner, J. *J. Phys. Chem. B* **2000**, *104*, 9740. (g) Grozema, F. C.; Berlin, Y. A.; Siebbeles, L. D. A. *J. Am. Chem. Soc.* **2000**, *122*, 10903. (h) Berlin, Y. A.; Burin, A. L.; Ratner, M. A. *J. Am. Chem. Soc.* **2001**, *123*, 260.
5. (a) Nunez, M. E.; Hall, D. B.; Barton, J. K. *Chem. Biol.* **1999**, *6*, 85. (b) Ly, D.; Sanii, L.; Schuster, G. B. *J. Am. Chem. Soc.* **1999**, *121*, 9400.
6. (a) Lewis, F. D.; Liu, X. Y.; Liu, J. Q.; Miller, S. E.; Hayes, R. T.; Wasielewski, M. R. *Nature* **2000**, *406*, 51. (b) Lewis, F. D.; Liu, J. Q.; Zuo, X. B.; Hayes, R. T.; Wasielewski, M. R. *J. Am. Chem. Soc.* **2003**, *125*, 4850.
7. (a) Pollard, W. T.; Felts, A. K.; Friesner, R. A. *Adv. Chem. Phys.* **1996**, *93*, 77. (b) Priyadarshy, S.; Risser, S. M.; Beratan, D. N. *J. Phys. Chem.* **1996**, *100*, 17678. (c) Okada, A.; Chernyak, V.; Mukamel, S. *J. Phys. Chem. A* **1998**, *102*, 1241. (d) Henderson, P. T.; Jones, D.; Hampikian, G.; Kan, Y.; Schuster, G. B. *Proc. Natl. Acad. Sci. U.S.A.* **1999**, *96*, 8353.
8. (a) Diederichsen, U. *Angew. Chem., Int. Ed. Engl.* **1996**, *35*, 445. (b) Diederichsen, U. *Bioorg. Med. Chem. Lett.* **1997**, *7*, 1743. (c) Diederichsen, U. *Angew. Chem., Int. Ed. Engl.* **1997**, *36*, 1886.
9. Diederichsen, U. In *Perspectives in Bioorganic Chemistry*; Diederichsen, U.; Lindhorst, T. K.; Westermann, B.; Wessjohann, L. A., Eds.; Wiley-VCH, Weinheim, 1999; p 255.
10. Weicherding, D.; Diezemann, N. J.; Vockelmann, E.; Diederichsen, U., manuscript in preparation.
11. Diederichsen, U.; Weicherding, D. *Synlett* **1999**, 917.
12. AlaG = β-(guanin-9-yl)alanine, AlaC = β-(cytosin-1-yl)-alanine, AlaA = β-(adenin-9-yl)alanine, AlaT = β-(thymin-1-yl)alanine; D-configurated nucleo amino acids are underlined.
    The synthesis of the nucleo amino acids, of the acridine derivative and of the oligomers **1–4** as well as the temperature dependent UV-spectroscopy were performed as described previously.[7,10] Oligomers **5** and **6** were prepared in analogy. **5**: ESI-MS *m/z* (%): 756.0 (100) $[M+2H]^{2+}$, 1510.3 (20) $[M+H]^+$; **6**: ESI-MS *m/z* (%): 760.5 (100) $[M+2H]^{2+}$, 1519.4 (37) $[M+H]^+$.
13. Steenken, S.; Jovanovic, S. V. *J. Am. Chem. Soc.* **1997**, *119*, 617.
14. Seidel, C. A. M.; Schulz, A.; Sauer, M. H. M. *J. Phys. Chem.* **1996**, *100*, 5541.